



Visible-light promoted fluoroalkylselenolation: toward the reactivity of unsaturated compounds†

Clément Ghiazza,^a Lhoussain Khrouz,^b Cyrille Monnereau,^b
Thierry Billard^{*a,c} and Anis Tlili^{*a}

Cite this: *Chem. Commun.*, 2018,
54, 9909

Received 30th June 2018,
Accepted 6th August 2018

DOI: 10.1039/c8cc05256e

rsc.li/chemcomm

The reactivity of fluoroalkylselenotoluenesulfonates with unsaturated substrates is explored herein. The direct activation of these shelf-stable reagents under visible light allows the double functionalisation of alkenes or alkynes efficiently, leading to a wide range of β -fluoroalkylselenolated sulfones. Mechanistic investigations have been undertaken supporting the formation of radical intermediates.

The formation of trifluoromethylchalcogen–carbon bonds has gained widespread interest during the past few years.^{1–12} The high lipophilicity^{13,14} of the trifluoromethylchalcogen groups is the most desirable benefit to the corresponding molecules. In this context several advances have been made for the formation of C–OCF₃^{1–3} as well as C–SCF₃ bonds.^{4–10} More recently, attention has been turned to the C–SeCF₃ bond formation process.^{11,12} Herein such transformation has been scarcely investigated mainly due to a lack of reagent development. In this context, our group has been involved in the synthesis as well as the application of a new family of shelf-stable electrophilic reagents, namely, fluoroalkylselenotoluenesulfonates.^{15–17} These reagents have already been successfully employed for electrophilic trifluoromethylselenolations for the formation of C(sp₂)–SeCF₃^{15,16} as well as C(sp)–SeCF₃ bonds under copper catalysis.¹⁷

Previous results in the literature have demonstrated radical homolyses of fluorinated thiosulfonates (SO₂–S bond)^{18–21} and fluorinated selenosulfonates (SO₂–Se bond).^{18,22} Moreover, in a continuity in the exploration of these reactions, we demonstrated that the homolysis of the S–Se bond in fluoroalkylselenotoluenesulfonates could take place at room temperature upon visible light activation in DMSO (Fig. 1).²³

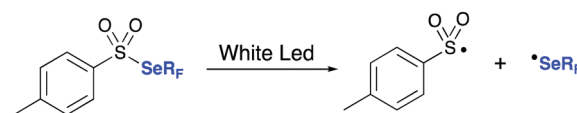


Fig. 1 Homolysis of the S–Se bond under visible light.

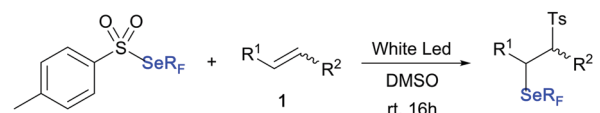
With this result in hand, we envisioned to evaluate the reactivity of the generated radicals from fluoroalkylselenotoluenesulfonates upon irradiation in the presence of unsaturated compounds (alkenes and alkynes). The first test has been performed with styrene **1a** and TsSeCF₃ (**1**). To our delight, the reaction provides the addition product **2a** with an excellent yield of 95% within 3 hours. A blank reaction performed in the absence of the white LED lamp obviously demonstrated the necessity of the irradiation to trigger the reaction outcome since no product was detected. Similarly, under thermal activation (50 °C), product **2a** was formed with a quite low yield of 31%. Following those initial investigations, we focused at expanding the reaction-scope using various alkenes (Scheme 1). In general, the yields were very good for styrene derivatives substituted in the *para* position (**2b–c**) as well as with internal alkenes. Indeed, the product arising from anethol (**2d**) was formed with a total regio- and diastereoselectivity with an excellent yield of 87%. The X-ray analysis of **2d** has confirmed the obtained structure. This diastereoselectivity can be rationalized essentially by the steric hindrance of the tosyl moiety which would hamper the approach of the CF₃Se species and, consequently, would favour an anti approach. Furthermore, aliphatic alkenes were also successfully converted to their corresponding products in quantitative yields under the same reaction conditions (**2e–g**). An excellent regioselectivity could be also observed with these compounds. In contrast, a moderate yield was obtained with dihydropyran **1h**, but always with an excellent *trans*-diastereoselectivity (confirmed by X-ray analysis). Interestingly, (*E*)- or (*Z*)-oct-4-enes **1i** lead to the same mixture of diastereoisomers (**2i**, **2i'**) in a similar ratio (around 85 : 15), indicating that the products evolved from the same planar radical intermediate. Finally, we also investigated the reactivity with higher

^a Institute of Chemistry and Biochemistry (ICBMS – UMR CNRS 5246), Univ. Lyon, Université Lyon 1, CNRS, 43 Bd du 11 novembre 1918, F-69622 Villeurbanne, France. E-mail: thierry.billard@univ-lyon1.fr, anis.tlili@univ-lyon1.fr

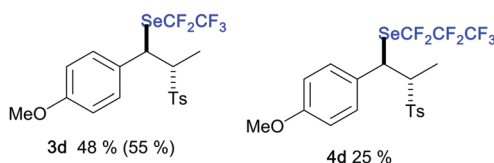
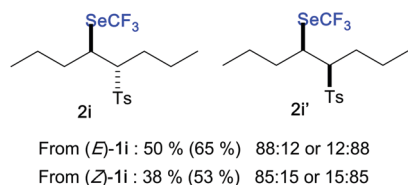
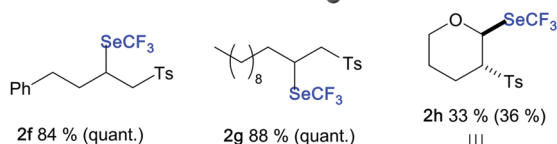
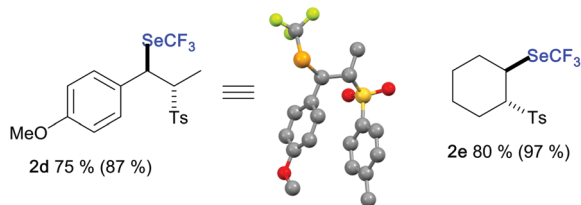
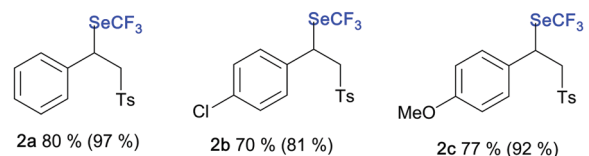
^b Univ Lyon, ENS de LYON, CNRS UMR 5182, Université Lyon 1, Laboratoire de Chimie, F-69342, Lyon, France

^c CERMEP – in vivo imaging, Groupement Hospitalier Est, 59 Boulevard Pinel, F-69003 Lyon, France

† Electronic supplementary information (ESI) available. CCDC 1847306–1847308. For ESI and crystallographic data in CIF or other electronic format see DOI: 10.1039/c8cc05256e



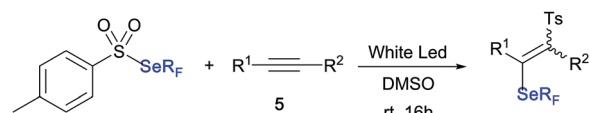
- I $R_F = CF_3$ 2 $R_F = CF_3$
 II $R_F = CF_2CF_3$ 3 $R_F = CF_2CF_3$
 III $R_F = CF_2CF_2CF_3$ 4 $R_F = CF_2CF_2CF_3$



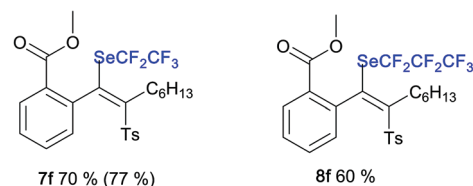
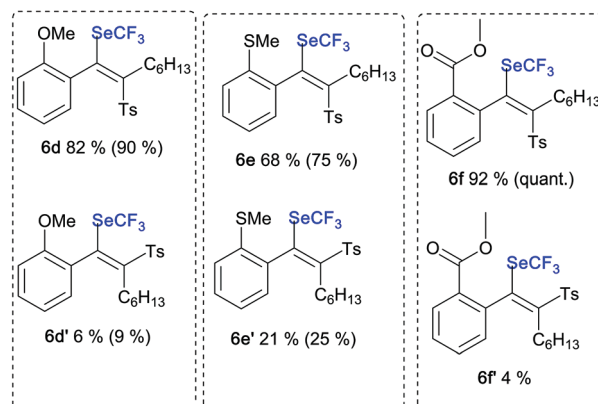
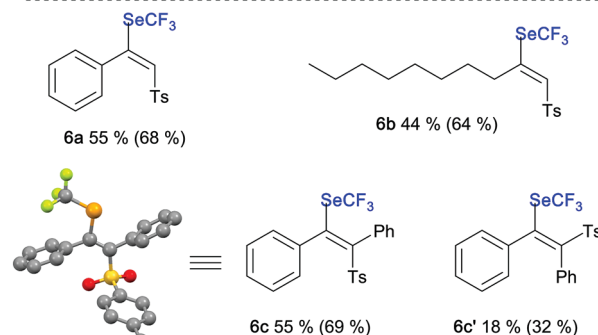
Scheme 1 Addition of $TsSeR_F$ into alkene derivatives. Reactions were performed with $TsSeR_F$ (0.25 mmol, 1.25 equiv.), alkene (0.2 mmol, 1 equiv.) and DMSO (1.5 mL). The reaction mixture was stirred at room temperature for 16 hours under white LED irradiation. Yields shown are those of isolated products; yields determined by ^{19}F NMR spectroscopy are shown in parentheses.

homologs: β -perfluoroalkylselenolated sulfones were prepared in synthetically useful (**4d**) to moderate yields (**3d**).

After having established the versatility and robustness of the reaction with alkenes, we turned our attention to expand its scope to alkynes. Terminal aromatic as well as aliphatic alkynes were evaluated at first. Phenylacetylene **5a** and dec-1-yne **5b** furnished the desired vinyl sulfones in 68% and 64% yields, respectively. Afterwards, we evaluated di-substituted alkynes. With diphenylacetylene **5c**, two stereoisomers were separated and characterized. The X-ray analysis confirmed the (*E*)-vinyl sulfone **6c** as the major product. Dissymmetrical alkynes bearing aromatic and aliphatic side chains were also engaged. A total



- I $R_F = CF_3$ 6 $R_F = CF_3$
 II $R_F = CF_2CF_3$ 7 $R_F = CF_2CF_3$
 III $R_F = CF_2CF_2CF_3$ 8 $R_F = CF_2CF_2CF_3$



Scheme 2 Addition of $TsSeR_F$ into alkyne derivatives. Reactions were performed with $TsSeR_F$ (0.25 mmol, 1.25 equiv.), alkyne (0.2 mmol, 1 equiv.) and DMSO (1.5 mL). The reaction mixture was stirred at room temperature for 16 hours under white LED irradiation. Yields shown are those of isolated products; yields determined by ^{19}F NMR spectroscopy are shown in parentheses.

conversion was reached independent of the aromatic substituent nature (electron withdrawing or donating groups). In all cases, the thermodynamically more stable (*E*)-product was predominantly formed. This methodology was also extended to perfluoroalkyltolueneselenosulfonates with very good yields (**7f**, **8f**). In these cases, only traces of (*Z*)-isomers were detected in the crude mixture (but not isolated) (Scheme 2).

Mechanistic studies were then performed to get knowledge of the reaction pathway. Firstly, in the presence of TEMPO (((2,2,6,6-tetramethylpiperidin-1-yl)oxyl)) the reaction did not give rise to the expected product. Secondly, controlled UVA

(380 nm) irradiation of a reaction medium containing reagent **I** and styrene in DMSO in similar concentration as depicted in the Experimental section (see also ESI† for detailed irradiation protocol) was performed and monitored over time by ^{19}F NMR spectroscopy, UV-vis absorption spectroscopy and ESR spectroscopy.

^{19}F NMR monitoring of aliquots taken off the reaction medium after different irradiation periods showed progressive disappearance of reactant **I** and concomitant formation of product **2a**. Comparison of the respective integrations of the reactant and product allowed a conversion degree to be established for each irradiation time which we could correlate to a photochemical quantum yield of product formation of *ca.* 7.8 (780%) following the methodology depicted in ESI†. This value unambiguously rules out the possibility of a step-wise mechanism and is in agreement with a chain mechanism induced by an initial photoinduced dimerization of reactant **I**.

As a further support to this hypothesis, a progressive decay of the absorption band corresponding to reagent **I** could also be monitored over time by UV-vis absorption spectroscopy, following a trend that could be fitted to a pseudo first order kinetic (see ESI† for protocols and illustrations). Similarly, plotting of the decay of the 385 nm absorbance *versus* irradiation time was used to determine the temporal conversion efficiency in the medium, and thus to establish, following a protocol detailed in the ESI†, a quantum yield of *ca.* 10.3 (1030%) which, within experimental error, is in line with the conclusion drawn from the NMR experiments and reinforces the hypothesis of a chain propagation mechanism starting with photodecomposition of reagent **I**.

Note that the discrepancies observed between the photochemical quantum yields as calculated by NMR and UV-vis can arise from: (i) the fact that NMR aliquots were immediately diluted *ca.* 1000 fold in CDCl_3 , thereby “freezing” the propagation reaction, while chain propagation could proceed and increase reactant conversion in the course of the UV-vis measurement; (ii) the fact that UV-vis measurement monitors the disappearance of reagent **I** only, while NMR focuses on the amount of product **2a**: for the latter, we neglect in the estimation of photochemical quantum yield, the build-up of the intermediate selenium dimer (which is the real product of the photochemical reaction, *vide infra*, and which is clearly seen in the NMR spectra) and its kinetics of transfer onto the styrene molecule.

ESR experiments were then conducted to confirm the nature of the radical intermediates involved in the reaction sequence. PBN was first used as a radical scavenger: when irradiation was performed in the absence of styrene, no significant ESR signal was observed. This leads us to postulate that the radicals observed in the following most likely correspond to PBN adducts of intermediates **A** and **B**. Upon addition of styrene and subsequent irradiation, a characteristic temporal evolution was seen on intermediate **B**. In the first few minutes of photoirradiation, an ESR signal gradually increases, witnessing the progressive formation of a first paramagnetic species. Its signature, featuring a characteristic $a_{\text{N}} = 13.6$ G and $a_{\text{H}} = 1.6$ G is in line with addition of a selenium centred radical onto the scavenger. From the above-mentioned arguments, **B** appears as the most likely hypothesis, although the g and a values could also correspond to a $\text{CF}_3\text{Se}^\bullet$ radical

(which builds up in the course of the chain propagation mechanism), or even to an overlay of both species. The intensity of this signal then gradually decreases, while a new signal ($a_{\text{N}} = 15$ G $a_{\text{H}} = 2.9$ G) appears. Its features are consistent with the formation of the carbon-centred **A** radical that evolves during the chain propagation reaction. Addition of the latter onto the scavenger apparently occurs at a slower rate than that of **B**, hence the delayed appearance of the signal. Conversely, temporal stability of the resulting adduct is higher, since the signal steadily increases and no decay is observed until irradiation is stopped. Similar experiments performed with DMPO as a radical scavenger (see ESI†) lead to similar conclusions, although the intensity of the first generated species (corresponding to **B**) is relatively much weaker, likely witnessing a more efficient addition of the **A** species onto the DMPO radical scavenger (Fig. 2).

Altogether, these mechanistic investigations lead us to propose the following mechanism, as depicted in Scheme 3. The irradiation of reagent **I**, in DMSO, leads to homolysis of the S–Se bond. The resulting toluenesulfonyl radical adds onto the double bond of styrene (**1a**), resulting in the radical intermediate **A**, while the selenium containing radical dimerizes to form $(\text{CF}_3\text{Se})_2$, as observed by ^{19}F NMR monitoring and as previously demonstrated.²³ This dimer adds onto the benzylic radical of intermediate **A**, to afford

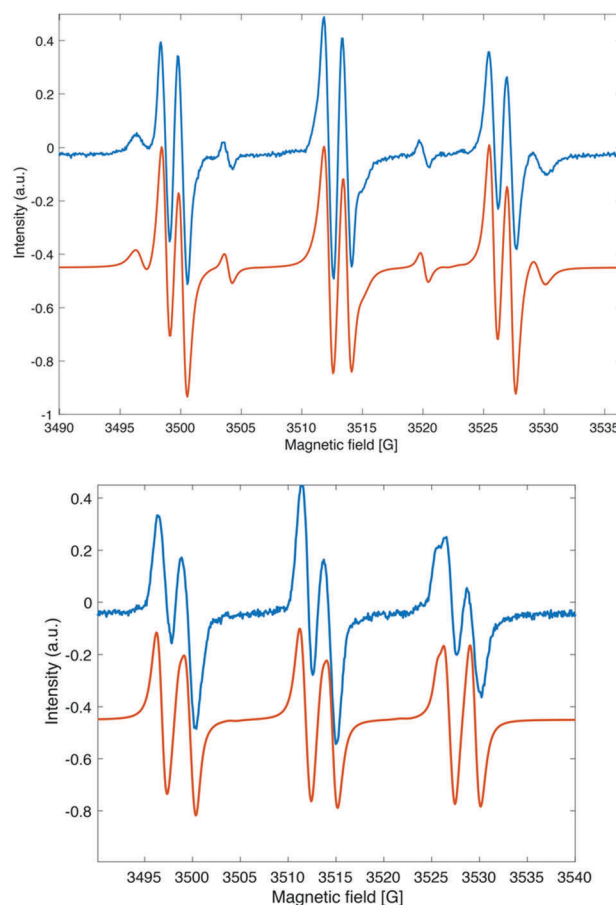
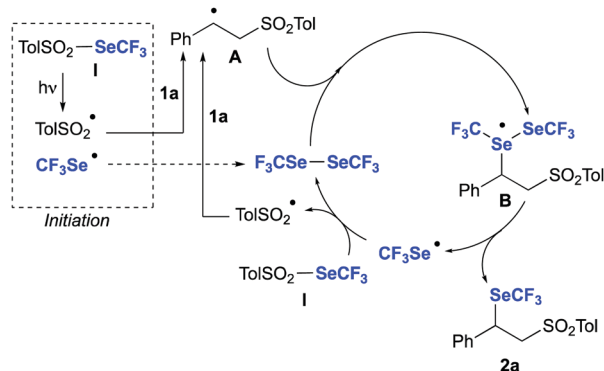


Fig. 2 ESR spin-trapping spectra on visible irradiation in the presence of PBN in DMSO at room temperature. Blue: experimental, and red: simulated after 3 minutes (top) and 7 minutes (bottom) of irradiation.



Scheme 3 Proposed mechanism.

intermediate **B**. Intermediate **B** evolves into the final product, by release of a selenium radical which in turn reacts with reagent **I**. This results in the formation of a new selenium dimer and of the sulfonyl radical, which initiates the chain propagation process.

To conclude, we herein demonstrated that the shelf-stable fluoroalkylselenotoluenesulfonates could react, upon activation with visible light, with unsaturated compounds (alkenes and alkynes) in a stereo- and regioselective way under mild conditions. The key step herein is the homolysis of the S–Se bond leading to new radical active species. Initial mechanistic studies allowed us to firmly establish that reaction further proceeds through a chain propagation mechanism. Using this standard synthetic protocol, higher homologs were also tolerated allowing us to considerably expand the scope of accessible products, carrying a large variety of chemical functions. Further developments are under investigation in our laboratory.

Conflicts of interest

There are no conflicts to declare.

Notes and references

- 1 F. R. Leroux, B. Manteau, J.-P. Vors and S. Pazenok, *Beilstein J. Org. Chem.*, 2008, **4**, 13.
- 2 T. Besset, P. Jubault, X. Pannecoucke and T. Poisson, *Org. Chem. Front.*, 2016, **3**, 1004–1010.
- 3 A. Tlili, F. Toulgoat and T. Billard, *Angew. Chem., Int. Ed.*, 2016, **55**, 11726–11735.
- 4 V. N. Boiko, *Beilstein J. Org. Chem.*, 2010, **6**, 880–921.
- 5 A. Tlili and T. Billard, *Angew. Chem., Int. Ed.*, 2013, **52**, 6818–6819.
- 6 F. Toulgoat, S. Alazet and T. Billard, *Eur. J. Org. Chem.*, 2014, 2415–2428, DOI: 10.1002/ejoc.201301857.
- 7 X.-H. Xu, K. Matsuzaki and N. Shibata, *Chem. Rev.*, 2015, **115**, 731–764.
- 8 S. Barata-Vallejo, S. Bonesi and A. Postigo, *Org. Biomol. Chem.*, 2016, **14**, 7150–7182.
- 9 H.-Y. Xiong, X. Pannecoucke and T. Besset, *Chem. – Eur. J.*, 2016, **22**, 16734–16749.
- 10 F. Toulgoat and T. Billard, in *Modern Synthesis Processes and Reactivity of Fluorinated Compounds: Progress in Fluorine Science*, ed. H. Groult, F. Leroux and A. Tressaud, Elsevier Science, London, United Kingdom, 2017, ch. 6, pp. 141–179.
- 11 Z. Cai, *J. Chin. Chem. Soc.*, 2017, **64**, 457–463.
- 12 A. Tlili, E. Ismalaj, Q. Glenadel, C. Ghiazza and T. Billard, *Chem. – Eur. J.*, 2018, **24**, 3659–3670.
- 13 A. Leo, C. Hansch and D. Elkins, *Chem. Rev.*, 1971, **71**, 525–616.
- 14 B. Linclau, Z. Wang, G. Compain, V. Paumelle, C. Q. Fontenelle, N. Wells and W.-W. Alex, *Angew. Chem., Int. Ed.*, 2016, **55**, 674–678.
- 15 Q. Glenadel, C. Ghiazza, A. Tlili and T. Billard, *Adv. Synth. Catal.*, 2017, **359**, 3414–3420.
- 16 C. Ghiazza, A. Tlili and T. Billard, *Beilstein J. Org. Chem.*, 2017, **13**, 2626–2630.
- 17 C. Ghiazza, V. Debrauwer, T. Billard and A. Tlili, *Chem. – Eur. J.*, 2018, **24**, 97–100.
- 18 T. Billard, N. Roques and B. R. Langlois, *J. Org. Chem.*, 1999, **64**, 3813–3820.
- 19 H. Li, C. Shan, C.-H. Tung and Z. Xu, *Chem. Sci.*, 2017, **8**, 2610–2615.
- 20 B. Xu, D. Wang, Y. Hu and Q. Shen, *Org. Chem. Front.*, 2018, **5**, 1462–1465.
- 21 S.-H. Guo, X.-L. Zhang, G.-F. Pan, X.-Q. Zhu, Y.-R. Gao and Y.-Q. Wang, *Angew. Chem., Int. Ed.*, 2018, **57**, 1663–1667.
- 22 T. Billard, B. R. Langlois and S. Large, *Phosphorus, Sulfur Silicon Relat. Elem.*, 1998, **136**, 137 & **138**, 521–524.
- 23 C. Ghiazza, V. Debrauwer, C. Monnereau, L. Khrouz, M. Médebielle, T. Billard and A. Tlili, *Angew. Chem., Int. Ed.*, 2018, DOI: 10.1002/anie.201806165.